The numerical simulation for the unsteady heat and mass transfer process in capillary pumped loops evaporator

HAN Yan-min, LIU Wei, HUANG Xiao-ming
(Department of Power Engineering Huazhong University of Science and Technology, Wuhan 430074, China)

Abstract: The flow in the porous medium is modeled by using the Brinkman-Forchheimer extended Darcy model based on the volume averaging of microscopic conservation equations. For the liquid-saturated layer and the vapor-saturated layer, the two sets of equations coupled with the matching conditions at the liquid-vapor interface are developed. The unsteady state calculations with methanol as a working fluids at different heat loads allow us to trace the evolution phases in the porous wick of a CPL evaporator: growth of vapor zones from origin. Detailed results of the evolution of pressure and heat are provided. The results indicate that at the initialization of start-up process, the low heat load exerted on the evaporator is suggested in order to avoid the dry-out situation in the porous wick. Adopting warm-up device to improve the vapor outlet condition in the vapor groove will increase the steady characteristic after start-up or with working condition variation. The analysis of evaporator of CPL system based on the numerical calculation will offer an important direction to the CPL design and system optimization.

Key words: Capillary pumped loops; Evaporator; Saturated porous wick; Liquid-vapor interface; Non-steady; Numerical simulation

CLC number: TK124 **Document code**: A **Article ID**: 1000-1328(2003)04-0397-07

0 Introduction

With high efficiency, dependability, and energy saving, the Capillary Pumped Loop, as a two-phase heat transfer system, drives the working-media circulation with the surface tension. The CPL can be applied in many fields such as in cooling high power density electronic devices, controlling heat transfer on aircraft and so on. Cao and Faghri[1] developed an analytical solution of two-dimensional model and later presented numerical simulations on three-dimensional model by conjugate analysis including a segment of wick and a groove. This solution is however restricted to homogeneous wicks and situations in which the wick is completely saturated with liquid. This study was restricted to situations where the phase change takes place at the groove wick interface and not within the wick. Demidov and Yatsenko[2] firstly presented a numerical study showing that vapor zones can take place within the wick under the fin. These studies display the liquid-vapor interface change in capillary porous media, the character of the pressure-field and evaporating quantity of evaporator outlet. C. Figus and Y. Le Bray[3] considered the capillary zone in the evaporator as the liquid-saturated layer and the vapor-saturated layer, their study presented the solutions on the processing of heat and mass transfer in the porous wick under the saturated assumption. Based on the case that the continuum approach to porous media is not adapted for modeling a system close to a percolation threshold, they developed a pore network model to predict the fractal patterns of the invasion percolation type. With the steady models they used on capillary study, the CPL non-steady characteristics including start-up and operation are not displayed with the variations of conditions. Muraoka[4] developed a mathematical

收稿日期: 2002-11-11, 修回日期: 2003-05-06。
基金项目: 国家重点基础研究发展规划(No. G2000026303)资助项目

model for describing the transportation of heat and mass inside the loop during all its operational regimes based on the nodal method.

When the parameter such as temperature the CPL non-steady operation educing deviating from its normal value or displays continual oscillation characteristic after start-up or working condition change, the CPL system is then defined as in non-steady operation state. It is of great significance to find out the factors which inducing non-steady characteristics harmful to system operations[5~7]. In this paper, the analysis of evaporator of CPL system based on the numerical calculation will offer important directions in controlling and removing the harmful influence, also in the CPL design and system optimization.

1 Physical model

Due to the symmetry of the evaporator fins of the CPL system (shown in Fig. 1), the study is restricted to a segment of the wick as sketched, a two-dimensional geometry is considered domain marked (ABCDE). The upper of the typical computational domain is the highly density heat flux from the evaporator fin, the left (AE) and the right (CD) of the domain is under symmetry condition, and bottom of the domain (ED) is the liquid compensation cavity. The vapor flowing through the grooves towards the condenser and condensed liquid returning to the evaporator are derived from the capillary pressure cross the surface tension formed at the interface of the liquid-vapor interface. The size of the evaporator is $200 \times 150 \times 20$ (mm^3), and there are 29 grooves inside. the dimension of the geometry is 5×5 (mm^2) that was used as the coordinates in the calculation procession. The wick porosity $\Phi$is 0.611(ϵ= 0.389), considering the heat transfer conditions, we use methanol (Evaporate Temperature is 337.15K) as working fluids. Under the laboratory condition, the condenser is cooled by water. At the start-up, the liquid in the porous media is considered as saturated, during the procession of start-up, the bottom temperature of the porous layer (the inlet temperature) keeps the constant and is set as 335.15K.

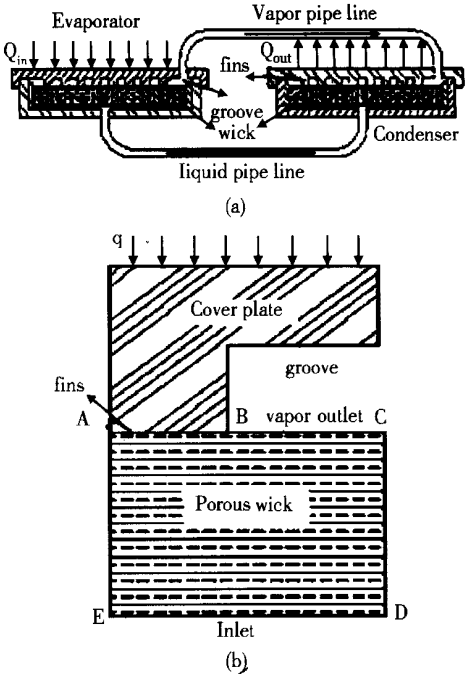

Fig. 1 Sketch of the CPL system (a) and the Physical domain (b)

2 Mathmetic model[8,9]

The flow in the porous medium is modeled by using the Brinkman-Forchheimer extended Darcy model based on the volume averaging of microscopic conservation equations. Considering the CPL working conditions, in the paper, we will neglect the affection of gravitation. Because the vapor is flowing into groove continuously, several assumptions are made in order to obtain a closed set of governing equations at macroscopic scale:

—the saturate vapor in the porous media;

—the local thermal equilibrium assumption;

—the viscous dissipation are negligible.

The governing equations are educed as follows:

(1) Vapor phase

Continuity equation

$$\frac{\partial(\epsilon_v \rho_v)}{\partial t} + \nabla \cdot (\rho_v \vec{V}_v) = 0$$

Momentum equation

$$\frac{\rho_v}{\epsilon_v}\frac{\partial \vec{V}_v}{\partial t}+\frac{\rho_v}{\epsilon_v^2}(\vec{V}_v\cdot\nabla)\vec{V}_v=-\nabla P_v-\frac{\mu_v}{K_v}\vec{V}_v+\frac{\mu_v}{\epsilon_v}\nabla^2\vec{V}_v$$

(2) Liquid phase

Continuity equation

$$\frac{\partial(\epsilon\rho_l)}{\partial t}+\nabla\cdot(\rho_l\vec{V}_l)=0$$

Momentum equation

$$\frac{\rho_l}{\epsilon}\frac{\partial \vec{V}_l}{\partial t}+\frac{\rho_l}{\epsilon^2}(\vec{V}_l\cdot\nabla)\vec{V}_l=-\nabla P_l-\left[\frac{\mu_l}{K_l}+\frac{\rho_l C}{K_l}\vec{V}_l\right]\vec{V}_l+\frac{\mu_l}{\epsilon}\nabla^2\vec{V}_l$$

(3) Energy equation of the porous media:

$$\bar{\rho}\bar{c}\frac{\partial T}{\partial t}+\rho_v c_v(\vec{V}_v\cdot\nabla)T+\rho_l c_l(\vec{V}_l\cdot\nabla)T=\nabla\cdot(k_{eff}\nabla T)$$

where the $\bar{\rho}\bar{c}=[\rho_l c_l\gamma+(1-\gamma)\rho_v c_v]\epsilon+(1-\epsilon)(\rho c)_s$, ϵ is the wick porosity, k_{eff} is the effective thermal conductivity, K is the permeability, γ is the liquid fraction in pore space, μ is viscosity. The subscript v stands for vapor, l stands for liquid, and s stands for solid. The energy equation should be satisfied the conjugate action between the two phase, so it is involved in the whole zone during the calculation.

2.1 Initial condition & Boundary conditions

In this study, the initial boundary conditions are mathematically expressed as

(1) Initial condition ($t=0$)

At time $t=0$, the porous media filled with saturated working fluent, that is:

$$\epsilon(t=0)=\phi=0.611.$$

The evaporator is at a uniform temperature $T_{in}=335.15$(K) and both the liquid and vapor velocities are zero.

(2) Boundary conditions ($t>0$)

At the bottom surface (D-E):

$$p_l=p_0,\ T_l=T_0$$

At the left and right surface(A-E, C-D):

$$\frac{\partial p}{\partial x}=0,\quad \frac{\partial T}{\partial x}=0$$

At the heating part of the top surface (A-B):

$$\frac{\partial p}{\partial y}=0,\quad \lambda\frac{\partial T}{\partial y}=q_W$$

At the wick outlet of the top surface (B-C):

$$\lambda\frac{\partial T}{\partial y}=\alpha(T_\infty-T),\ \lambda\frac{\partial T}{\partial y}=\frac{\rho LK}{\mu}\frac{\partial p}{\partial y}$$

At the surface of vapor and liquid layer:

$$T_l=T_v=T_{sat},\quad \rho_l\vec{V}_l=\rho_v\vec{V}_v$$

$$\lambda_v\nabla T_v\cdot n-\lambda_l\nabla T_l\cdot n=\rho_l\vec{V}_l\cdot nL,$$

$$p_c=p_v-p_l=2\sigma/r$$

where p_c is capillary pressure, L is the latent heat of vaporization, α is the heat transfer coefficient between the wick and the outlet vapor, the value was assumed to be $3\times10^5\,W\cdot m^{-2}\cdot K^{-1}$. Liquid is drawn from the bottom of the wick structure and flow to the liquid-vapor interface. The evaporator gradually reaches a steady state under the given conditions. At the wick outlet, the balance between the conduction heat from the wick and the latent heat of the working fluid is considered, and the heat is equal to the convective heat transfer.

2.2 Numerical procedure

The conservation equations and boundary conditions were solved by applying SIMPLE method (Semi-Implicit Method for Pressure-Linked Equations), the difficulty of attaining the front position was deal with a front tracking method, based on a moving structured grid that progressively adjusts to the front shape. This implies to regenerate the grids at each step according to the surface moving. The overall numerical procedure can be summarized as: Specifying an initial arbitrary liquid-vapor front location; Generating the grid; Solving the pressure Equation; Computing the velocity and the flow rate; Solving the energy Equation; Computing the new front location; Going back to generate the new grid; Repeating the procedure until convergence. A 25×25 elements grid turned out to be satisfactory.

3 Results and discussion

The numerical model was examined by checking the overall mass and energy balances over the simulation process. The unsteady state calculations

were first made with methanol as working fluid at different heat loads: q_e= 6kW · m^{-2} compared with q_e= 9kW · m^{-2} is applied. In the practical application, Because of the liquid occupying the vapor pipe, a warm-up device is usually installed in the system at the outlet of the CPL evaporator, at the start-up, the device can heat and turn the liquid into the vapor therefore improving the outlet conditions of vapor flowing into the groove. In this paper, the two situations with or without the warm-up device were performed in order to compare the results and find the essential reasons, so the optional design can be attained by analyzing the domain factors.

3.1 Results

Figure 2 and 3 show the temperature contours in $x-y$ planes, in the y direction, it gradually increases from the inlet temperature to the highest temperature at the inner surface of the cover plate fins. In the figure 2, the heat loads are 9 kw and the affection of the warm-up is negligible, while in the figure 3, the heat loads are 6 kw and the affection can't be neglected. The unsteady state at t= 10 min or t= 30 min show that the magnitudes of the temperature increase as it approaches to the liquid-vapor interface. The temperature contours in the figure 3 are more planar than in the figure 2, that is, the vapor in the wick can more easily emit out and flow in to the groove through the wider outlet. Adopting warm-up device to improve the vapor outlet condition in the vapor groove will increase the steady characteristic.

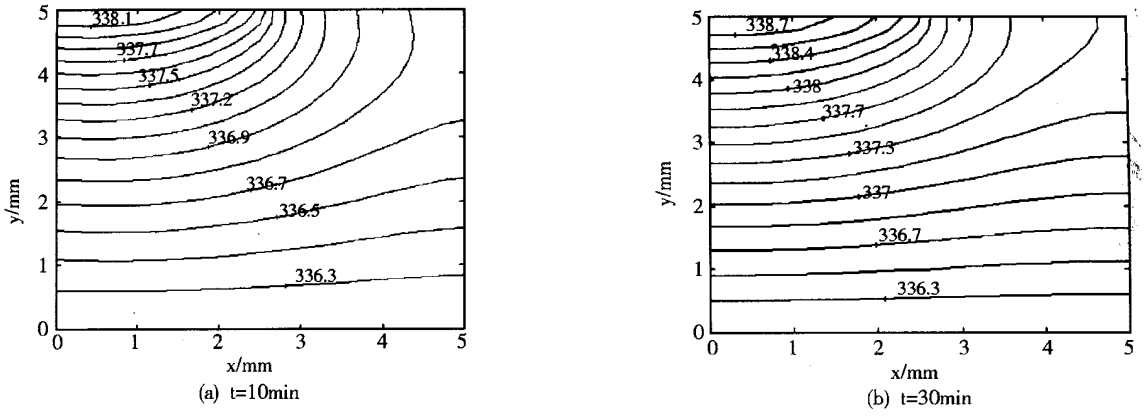

Fig. 2 Temperature field at q= 9kW · m^{-2}, without warm-up device

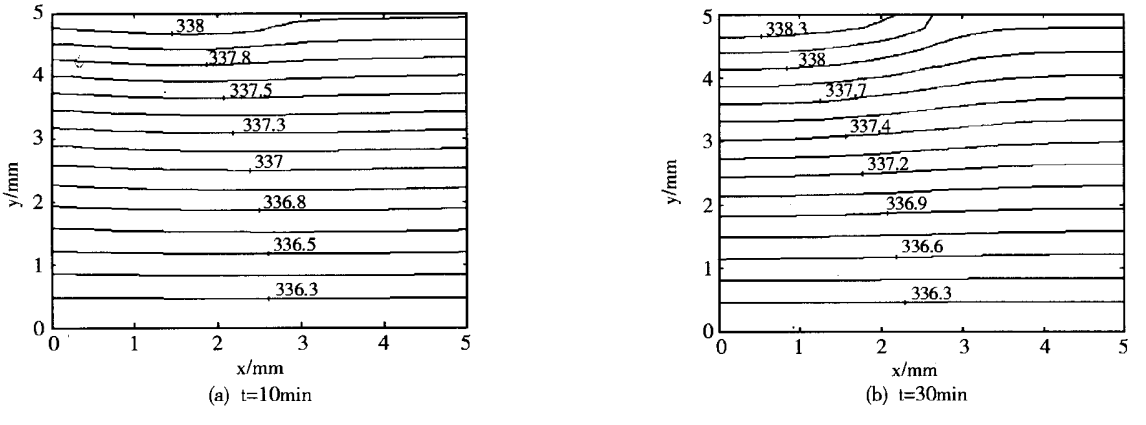

Fig. 3 Temperature field at q= 6kW · m^{-2}, with warm-up device

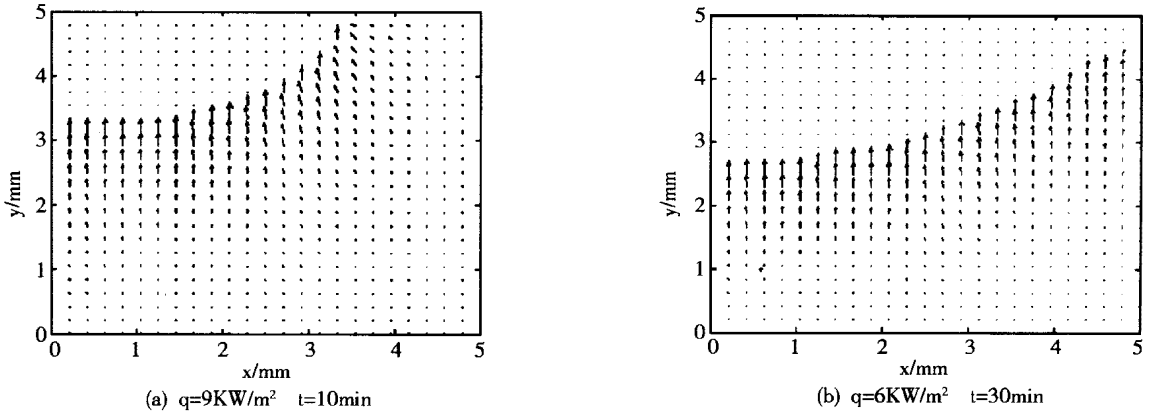

Fig. 4 Liquid velocity vectors in the porous wick

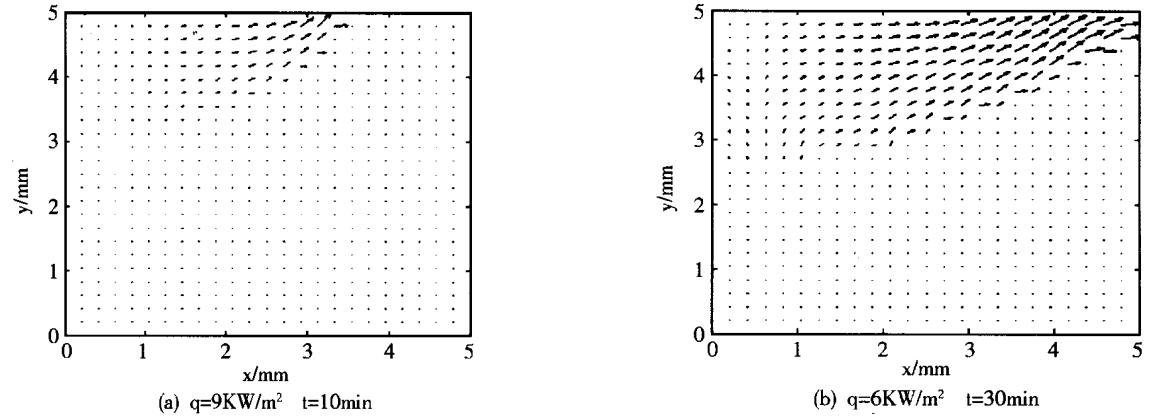

Fig. 5 Vapor velocity vectors in the porous wick

Figure 4 and 5 show the unsteady-state flow vector field in the $x-y$ plane at different time or different heat loads. Since the magnitudes of the liquid and vapor velocities are vastly different, the vector velocities of liquid or vapor phase are given in different figure. The magnitude of the liquid velocity increases as it approaches the liquid-vapor interface, also the magnitude of the vapor velocity increases as vapor travels down the groove, due to the mass accumulation at the vapor zone in the wick. Not surprisingly, the interface is gradually moving down into the wick as the time is prolonging, therefore, the vapor outlet dimension is also changing and the vapor outlet velocity is waving. As can be drawn out that the interface oscillation is one of the essential factors leading to the pressure waving in the system. At the unsteady-steady state, mass balances for liquid flow in the porous wick and vapor flow in the vapor zone are satisfied the continuum level. The moving velocity or the position of the predicted interface offers important limits in optimizing the heat loads or structure dimension. The results indicate that at the initialization of start-up process, the low heat load exerted on the evaporator is suggested in order to avoid the dry-out situation in the porous wick.

In the figure 6, the pressure contours show the liquid pressure in the wick structure. The vapor zone are saturated, the figure also shows the pressure drops in the wick structure. The maximum capillary pumping force available balances with the resistance of the whole system, the pressure difference between the interface and the position the pressure contours denoted are equal the flow resistance in the wick. The unsteady-state simulation describes the process how the initial state dis-

turbed by exterior conditions approaching to the new state. Figure 7 shows the temperature variation of the point nearby the vapor outlet during whole the unsteady process.

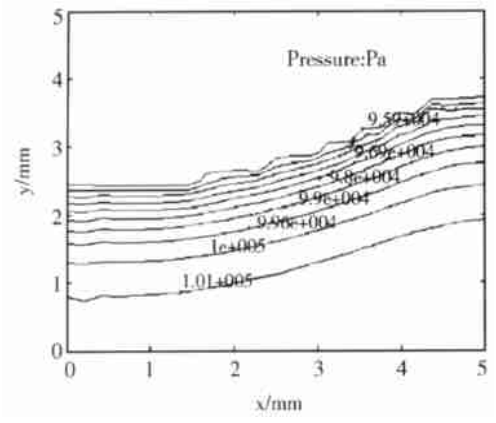

Fig. 6 Pressure distribution along the boundary of the computational domain ($q = 9kW/m^2$, $t = 40min$)

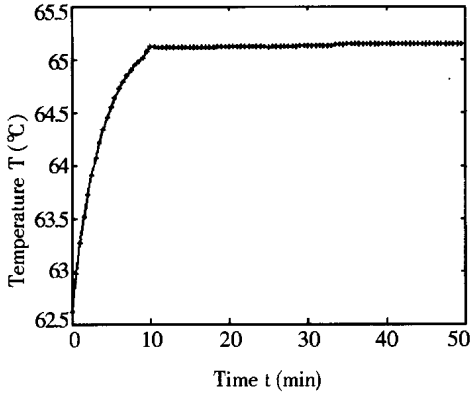

Fig. 7 Temperature variation of the point nearby the outlet during the unsteady process ($q = 9kW/m^2$, $t = 0 - 50$ min)

3.2 Conclusions

For the liquid-saturated layer and the vapor-saturated layer, the analysis of the unsteady-state simulation reveals such conclusions as follows: During the start-up process of the CPL system, the liquid-vapor interface is moving down into the wick with the prolongation of the time, and the vaporizing area and the dimension of the outlet is increasing. The initial heat load is one of the main factors in predicting the final position of the interface. Therefore, lower heat load is suitable to the initial state to avoid the interface surpass the limit of the porous wick. In or to enhance the system stability, such methods can be taken as optimizing the vapor outlet condition, groove and fins dimension. A warm-up device will be convenient for the system start by removing the liquid in the vapor pipe. The inlet temperature play a important role to the stability of the system, by reducing the inlet temperature, the over-heat vapor will be decreased, the heat loads that the system can undertake will be increased. The whole temperature variation in the evaporator is small because of the phase changing in it.

References:

[1] Cao Y, and Faghri A. Conjugate analysis of a flat-plate type evaporator for capillary pumped loops with three-dimensional vapor flow in the groove, Int. J Heat and Mass Transfer, 1994, 37(9): 401-409

[2] Demidov A S, etc. Investigation of heat and mass transfer in the evaporation zone of a heat pipe operating by the 'inverted meniscus' principle, Int. J Heat and Mass Transfer, 1994, 37: 2155-2163

[3] Figus C, Le Bray Y, Bories S, etc. Heat and mass transfer with phase change in a porous structure partially heated: continuum model and pore network simulations, Int. J Heat and Mass Transfer, 1999, 42: 2557-2569

[4] Muraoka I, etc. Experimental and Theoretical Investigation of a Capillary Pumped Loop with a Porous element in the Condenser, Int. Comm. Heat and Mass Transfer, 1998, 25(8): 1085-1094

[5] Zhang Jia-Xun, Hou Zeng-Qi. The Application of CPL Technique in Spacecraft, Journal of Engineering Thermophy, 1998, 22(3): 340-343

[6] Qu Wei, Liu Ji-Fu. study on starting characteristics of capillary pumped loop, journal of Harbin Institute of Technology, 1999, 31(4): 74-79

[7] Zhang Jia-Xun, Hou Zeng-Qi, etc. Theoretical Analysis of The Pressure Oscillation Phenomena in Capillary Pumped Loop, Journal of Thermo Science

[8] Nield D A and Bejan A. Convection in Porous Media, New York: Springer-Verlag, 1992

[9] Hadim A. Forced Convection in a Porous Channel With Localized Heat Sources, Transactions of the ASME, 1997, 116(5): 41-53

作者简介: 韩延民(1974-), 男, 硕士, 专业: 工程热物理; 研究方向: 多孔介质中的传热传质。

通讯地址: 华中科技大学能源与动力工程学院(430074)

电话: 027-87542618

CPL 蒸发器多孔芯内传热传质的非稳态数值模拟

韩延民，刘　伟，黄晓明

(华中科技大学能源与动力工程学院　武汉 430074)

摘　要: 基于多孔芯内局部热力学平衡的假设,考虑了 Brinkman 和 Forchheimer 对 Darcy 定律的修正模型,针对简化的物理模型中所包含的气液相区域,建立了二维分层饱和多孔介质模型,以甲醇为工质对 CPL 蒸发器毛细多孔芯内的传热传质过程进行非稳态数值模拟。在不同的热负荷条件下预测气液分层界面的形状和位置、系统由初态达到稳态过程的持续时间,讨论压力和温度的分布。由两层饱和模型所得到的计算结果可知: CPL 系统在启动时,为避免高热流时液体脱离多孔区而发生干涸,宜采用小负荷启动;采用预热器,改善蒸气的出口条件;增加蒸发器入口处的工质的过冷度,有利于增加CPL 系统启动过程和变工况时的稳定性。文中分析结论为 CPL 系统的优化设计提供参考。

关键词: CPL; 蒸发器; 饱和多孔芯; 气液分层界面; 非稳态; 数值模拟

中图分类号: TK124　　文献标识码: A　　文章编号: 1000-1328(2003) 04-0397-07

(上接第 377 页)

Study on a new type of continuous rotary electro-hydraulic servo motor applied to simulator

CAO Jian, LI Shang-yi, ZHAO Ke-ding

(School of mechanical and electrical engineering, Harbin Institute of Technology, Harbin 150001, China)

Abstract: The working principle of a new type of no-pulsation continuous rotary electro-hydraulic servomotor applied to simulator is introduced. The Lugre frication model used in this paper can meet the requirements for friction compensation of hydraulic system, because it could describe complex friction behavior, and two step off-line identification methodology of the Lugre parameters has been proposed. By way of experiment research, we have got a new type of friction model of continuous rotary motor, and the low speed and step response of the motor have been researched. Experimental results have proved that using fraction compensation could eliminate stick-slip motion at the low-speed and this servomotor could be applied to simulator.

Key words: Hydraulic servomotor; Frictional model; Frictional compensation; Experimental study